Distributions of rovibrational states of secondary product NO X 2 Π from photodissociation of nitric acid at 193 nm

Gen-Hou Leu and I-Chia Chen

Citation: The Journal of Chemical Physics **107**, 7223 (1997); doi: 10.1063/1.474963
View online: http://dx.doi.org/10.1063/1.474963
View Table of Contents: http://scitation.aip.org/content/aip/journal/jcp/107/18?ver=pdfcov
Published by the AIP Publishing

Distributions of rovibrational states of secondary product NO $X\ ^2\Pi$ from photodissociation of nitric acid at 193 nm

Gen-Hou Leu and I-Chia Chen[a)]
Department of Chemistry, National Tsing Hua University, Hsinchu, Taiwan 30043, Republic of China

(Received 27 May 1997; accepted 1 August 1997)

The distributions of vibrational, rotational, spin–orbit and lambda–doublet states of nascent NO are obtained using the $A\ ^2\Sigma - X\ ^2\Pi$ transition via the technique of laser-induced fluorescence. NO is produced mainly from secondary dissociation of fragment NO_2 from nitric acid after photolysis at 193 nm. According to the measured distribution the partition of energy in NO $X\ ^2\Pi$ is calculated to be $\sim 840\ cm^{-1}$ in vibration and $\sim 1410\ cm^{-1}$ in rotation. The spin–orbit state $^2\Pi_{1/2}$ of NO is populated about twice of that in $^2\Pi_{3/2}$ for the vibrational levels $v=0$, 1, and 2. The measured populations of vibrational states $v=0$, 1, and 2 are 0.75, 0.19, and 0.07, respectively; these populations agree with results calculated with the statistical model, prior theory. The distributions of rotational states of NO $X\ ^2\Pi$ for these three vibrational levels have single maxima of Gaussian shape. The experimental data indicate that although NO_2, produced photochemically from nitric acid, was proposed to be in an electronically excited state, the state distributions of NO from unstable NO_2 agree with those from NO_2 excited with monochromatic light in the UV-vis range after averaging for a broad distribution of internal energy. In the UV-vis range of excitation the NO fragment dissociates from the ground electronic surface of NO_2. Hence, this unknown electronic state of NO_2 is expected to be coupled to the ground electronic surface then leading to dissociation.
 [S0021-9606(97)00642-9]

I. INTRODUCTION

Solar photolysis of nitric acid is an important source of OH radicals in the stratosphere. Nitric acid also plays as a reservoir for NO_x in the atmosphere. Turnipseed *et al.*[1] have measured the quantum yield for the formation of OH using laser-induced fluorescence (LIF) to be 0.33 ± 0.06. Schiffman *et al.*[2] used direct infrared absorption to detect OH and found a quantum yield equal to 0.47 ± 0.06. Felder *et al.*[3] measured photofragment translational spectra of nitric acid and found the OH yield to be 0.6. Myers *et al.*[4] used similar technique with a different method to determine the OH yield and obtained 0.33 ± 0.04 for formation of NO_2 and OH, in agreement with the value of Turnipseed *et al.*[1] In addition, Myers *et al.*[4] reported yields 0.53 for singlet channel HONO $(\tilde{X}\ ^1A') + O(^1D)$ and 0.13 for triplet channel HONO $(\tilde{a}\ ^3A'') + O(^3P)$. Conclusively, one third of the product channels of nitric acid at 193 nm photolysis forms OH and NO_2. Felder *et al.*[3] and Myers *et al.*[4] found NO_2 formed from two pathways; one resulted in a stable electronic state whereas the other, about 69% of fragment NO_2, is unstable, undergoing secondary dissociation to NO+O. Dissociation to form NO_2 and OH requires energy $D_0 \approx 47.6\ kcal\ mol^{-1}$.[5] Hence, the fragment NO_2 can have energy that exceeds the dissociation energy, $25\,132\ cm^{-1}$ to produce NO+O.[6] Yeh *et al.*[7] observed emission of NO in the transition $D\ ^2\Sigma^+ - A\ ^2\Sigma^+$ in time-resolved Fourier-transform spectra; they concluded that NO formed in the first vibrationally excited state is a secondary fragment from NO_2 produced from nitric acid photolyzed at 193 nm. The product NO absorbed a second photon at 193 nm to the $D\ ^2\Sigma^+$ state. These photoproducts NO_x and HONO from nitric acid photolyzed in the UV range play important roles in the ozone cycle in the atmosphere; hence it is important to understand the photodissociation dynamics of nitric acid.

Previously[8] in this laboratory we found OH from nitric acid photolyzed at 193 nm to possess only 3% of available energy distributed to internal degrees of freedom of the OH fragment. The translational energies of OH and NO_2 are estimated from Doppler widths of OH and momentum conservation to be 2330 and $860\ cm^{-1}$, respectively, and 87.8% of the excess energy attributed to the internal energy of NO_2. In order to have so much energy and from the estimated distribution of internal energy, NO_2 is expected to be formed in an electronically excited state. Bai and Segal[9] suggested that the $NO_2\ ^2B_2$ state ($^2B_1$ shown in their paper which is incorrect[4]) is correlated to nitric acid $2\ ^1A'$, accessed by a 193 nm photon. Furthermore, Myers *et al.*[4] assigned stable NO_2 produced on photolysis of nitric acid to be in the $^2B_2$ state and unstable NO_2 to be in an unknown excited state lying above. Hence both experimental results and theoretical calculations indicate that NO_2 produced from nitric acid is in an electronically excited state. Because the strong vibronic interaction between the $^2B_2$ and the ground electronic state $^2A_1$, NO_2 initially formed in the $^2B_2$ state would undergo relaxation in a subpicosecond time scale to vibrationally excited states in the ground electronic surface with mainly electronic character of $^2A_1$.

The dissociation dynamics of NO_2 are investigated by many research groups.[6,10–33] Visible absorption spectra of NO_2 are complicated because of strong interactions among

[a)]Author to whom all correspondence should be addressed; E-mail address: icchen@faculty.nthu.edu.tw

the lowest electronic states. When an NO_2 molecule, prepared in a supersonic jet, is excited to exceed the dissociation threshold of formation of NO+O with a monoenergetic light, the rotational state distributions of NO fluctuate, but, on average, follow a statistical behavior.[16–18] In this work, nitric acid was photolyzed at 193 nm, and the state distributions of nascent NO were measured using LIF on the $A\ ^2\Sigma^+ - X\ ^2\Pi$ transition. Statistical models such as the prior theory[17] and separated statistical ensembles (SSEs)[34] are used to fit the experimental data. Internal state distributions of NO $X\ ^2\Pi$ produced photochemically from nitric acid and from photolysis of NO_2 directly in jet-cooled and thermalized conditions are compared.

II. EXPERIMENT

Fuming nitric acid with a purity greater than 99.5% (Merck), after degassing, flowed continuously through a gas cell at a pressure 20–30 mTorr and was photolyzed with an ArF excimer laser (Lambda Physik, Compex 100) at a wavelength 193 nm. The produced secondary photofragment NO was probed with LIF on the transition $A\ ^2\Sigma^+ - X\ ^2\Pi$. The probe beam is from a dye laser (Lambda Physik, LPD3002), pumped with an XeCl excimer (Lambda Physik, LPX220), after frequency doubling in a BBO crystal. The probe pulses, at a repetition rate 10 Hz, were collinear and delayed $\sim$50–150 ns after the photolysis pulses. The energy of the probe pulses was kept below 3 μJ/pulse (spot size 3 mm diam) to avoid saturation in exciting the $A\ ^2\Sigma^+ - X\ ^2\Pi$ transition. We ensured a single-photon process by checking the intensity ratio of the weak satellite peaks to that of the main branches of NO to be small. Only 50–100 μJ/cm^2 per pulse of an ArF excimer laser was used to photolyze nitric acid to avoid multiphoton processes occurring in dissociation of nitric acid. The power range of 10–200 μJ/cm^2 per pulse of 193 nm light was checked and found to be in the linear region of the LIF intensity of NO vs photolysis power. The total fluorescence of the excited NO was collected with a photomultiplier (PMT, Hamamatsu R212UH) after an interference filter [Corion (239$\pm$12) nm], mounted perpendicularly to both laser beams. The signal from the PMT was sent to a gated integrator, to an analog-to-digital ADC converter via a GPIB interface then to a personal computer for data processing.

Thermalized NO remaining in the gas cell interfered with detection of nascent NO in the vibrational ground state. Hence, during the scan we recorded a spectrum by alternating the probe pulses 100 ns before and after the photolysis pulses; from each data point was subtracted the background signal from NO taken before the photolysis pulses then averaged over 60 laser shots. After application of the subtraction, the uncertainty of spectral intensity for $J<15.5$ is too large to be included in the data. Spectra of NO $A\ ^2\Sigma^+ - X\ ^2\Pi$ (0,0), (0,1), and (0,2) bands were recorded and the intensity was normalized for fluctuations of both photolysis and probe pulses detected with photodiodes. About 30–50 laser shots were averaged for each data point. The ratios of spectral intensity between transitions from two

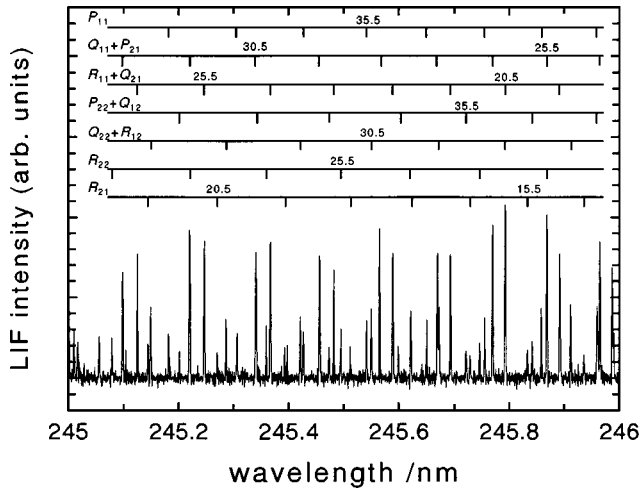

FIG. 1. Part of fluorescence excitation spectrum of nascent NO $A\ ^2\Sigma^+ - X\ ^2\Pi$, (0,2) transition produced on photodissociation of nitric acid at 193 nm.

vibrational levels of NO $X\ ^2\Pi$ were obtained on recording a long spectrum including parts of these two bands. Scans made on separate days were averaged to give the intensity ratios to determine the vibrational population of NO. Only the transitions from high rotational states of $v=0$ were used in determining the vibrational population of $v=0$.

III. RESULTS AND MODEL CALCULATIONS

A portion of the fluorescence spectrum and assignments for nascent NO in the $A\ ^2\Sigma^+ - X\ ^2\Pi$ (0,2) transition are shown in Fig. 1. The NO $X\ ^2\Pi$ state has two spin–orbit states $^2\Pi_{1/2}$ and $^2\Pi_{3/2}$; each of them has two lambda–doublet components. These components can be selectively detected on choosing different branches of transitions. In NO $A\ ^2\Sigma^+ - X\ ^2\Pi$, there are in total twelve branches. Limited by the experimental resolution, only eight branches are resolved; the Q_{11} branch overlaps with the P_{21} branch and Q_{22} with R_{12}. These overlapped branches are from the same lower state but to upper states that are spin components, only slightly split. The spectral intensities of transitions were divided by their Hönl–London factors[35] to obtain the relative rotational populations. All observed branches were analyzed to obtain the relative population of the NO states for the various lambda–doublet and spin–orbit states. Figure 2 shows a distribution of relative population of rotational states of $v=1$ obtained from eight branches of the (0,1) band. The population of the A'' component of $^2\Pi_{1/2}$ is determined from the spectral intensity of $Q_{11}+P_{21}$ and R_{21} and the A' component from P_{11} and $R_{11}+Q_{21}$, and analogously the A'' component of $^2\Pi_{3/2}$ from $Q_{22}+R_{12}$ and P_{12} and A' from $P_{22}+Q_{12}$ and R_{22}. The populations obtained from separate branches are approximately equal within the experimental error for the same spin–orbit state except for the $v=2$ level. The obtained populations for the same rotational state are averaged, and displayed in Fig. 3 for NO $X\ ^2\Pi$ $v=0$, 1, and 2 states. The populations for $J\leqslant 15.5$, $v=0$ are not shown in the plot because of a large experimental uncertainty arising

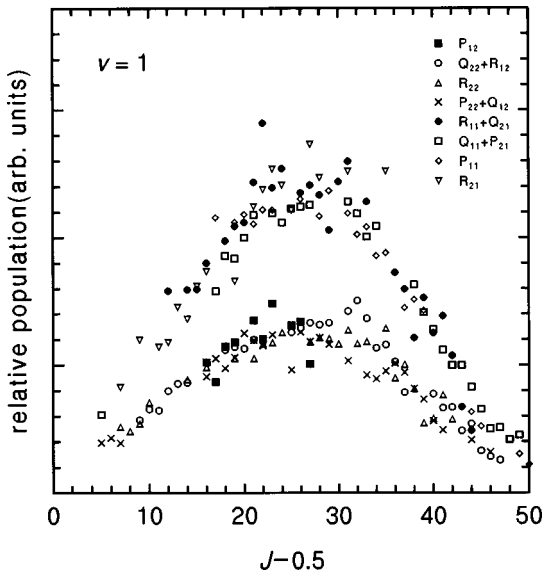

FIG. 2. Distributions of population of rotational states of nascent NO $X\ ^2\Pi$ $v=1$ obtained from various branches corrected for the rotational line strength.

from background NO remaining in the gas cell. For the measured vibrational states, the population of $^2\Pi_{1/2}$ is approximately twice of $^2\Pi_{3/2}$, shown in Fig. 4, although $^2\Pi_{1/2}$ is only 120 cm^{-1} lower in energy. These ratios ($\sim$1.9 on average) seem to be invariant with rotational quantum number. The maximal populations for the three vibrational levels are about $J=20.5-25.5$. The $v=2$ state has a smaller maximum J value $\sim$42.5 than the other vibrational states limited by the available energy, shown in Fig. 3. For $v=2$ state the observed population of the A' exceeds slightly than that of the A'' state but not for the other vibrational states. All rotational distributions of these three vibrational levels show a non-Boltzmann behavior (Fig. 5) and can be fitted with Gaussian functions (Fig. 3).

The population ratios among vibrational states were obtained on comparing the spectral intensities of transitions for various vibronic bands corrected for the Franck–Condon factors,[36] oscillator strengths, frequency factors, and weighted for the rotational population for that vibrational level. Because all three levels were obtained on exciting to the same upper level, there is no need to correct the spectral response of the detector and optical filters. In Table I we list experimental measurements for vibrational populations of NO $X\ ^2\Pi$. Vibrational levels up to $v=2$ were observed. Most NO produced was formed in the vibrational ground state, $\sim$75%. From the distributions of product states, the energy distributed in average to vibration of NO is $\sim$840 and $\sim$1410 cm^{-1} in rotation.

In previous work of photodissociation of HNO_3 at wavelength 193 nm,[8] the distribution of internal energy NO_2 was estimated from the Doppler widths of product OH transitions and from assuming conservation of momentum. In the same work, OH was formed in only the ground vibrational state

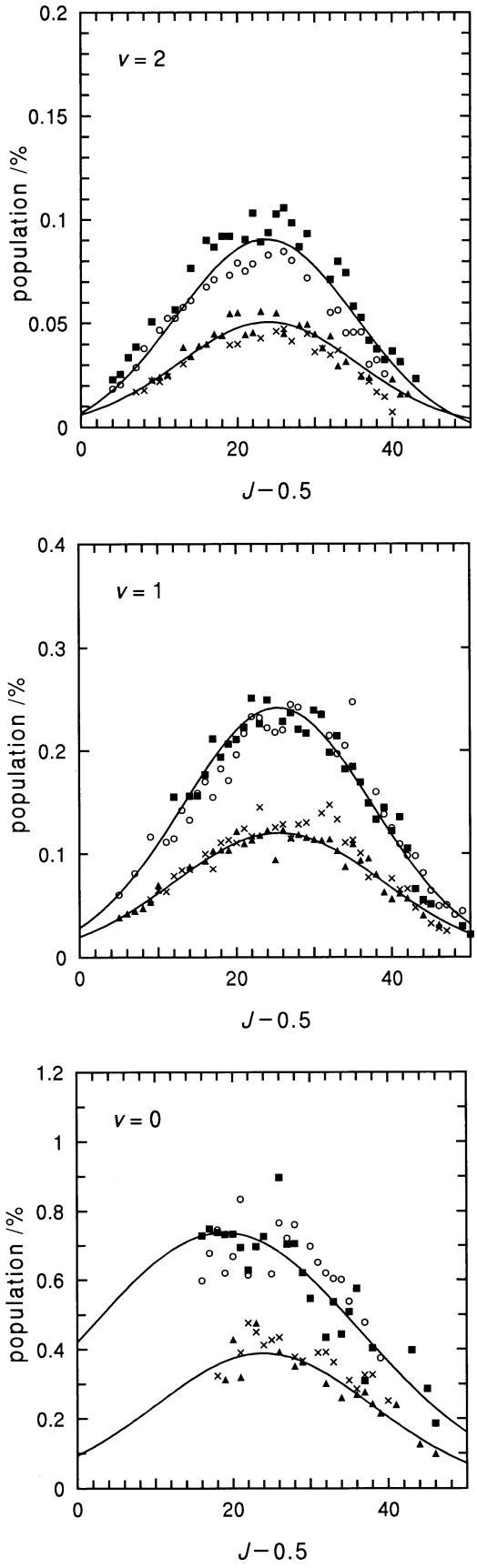

FIG. 3. Distributions of rotational states of nascent product NO $X\ ^2\Pi_{1/2}$ and $X\ ^2\Pi_{3/2}$ (a) $v=2$ (b) $v=1$, and (c) $v=0$ levels for lambda–doublet states A' (■) and A'' (○) of $^2\Pi_{1/2}$ and A' (×) and A'' (▲) of $^2\Pi_{3/2}$. The best-fit Gaussian functions for these distributions are displayed in solid line.

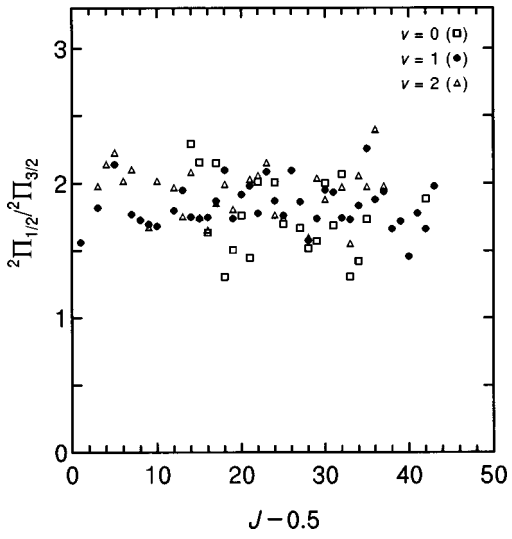

FIG. 4. Population ratio of NO $X\ ^2\Pi_{1/2}/X\ ^2\Pi_{3/2}$ as a function of NO rotational quantum number for three vibrational levels.

and with little rotational energy, indicating that much available energy is expected to be distributed as internal energy of the other fragment NO_2. The second distribution for the NO_2 internal energy, $P_{NO_2}(E_{int})$, was calculated from the distribution of translational energy, $P(E_t)$ obtained by Myers *et al.*[4] and the average internal energy of OH,[8] $E_{rot}(OH) = 950\ cm^{-1}$ given the relationship that $E_{int}(NO_2) \approx E_{ph} - E_{th} - E_{rot}(OH) - E_t$. The photon energy $E_{ph} = 51\,810\ cm^{-1}$ and the threshold energy of formation $NO_2 + OH$ from nitric acid is $E_{th} = 16\,660\ cm^{-1}$. The distribution from the OH Doppler width is expected to have a large experimental uncertainty because the Doppler width was obtained from convolution the spectral width of a transition with the laser width. The line shape of the laser beam was not purely Gaussian. Another assumption, that the velocity of the OH fragment is isotropic, was made. However, within the experimental uncertainties, the distributions from these two methods agree with each other, shown in Fig. 6. Nevertheless, the second method is a direct measurement of the translational energy; presumably, the distribution of internal energy of NO_2 is expected to be more accurate. Hence, we use this distribution to perform model calculations and compare the results from model calculations with the experimental data. According to the second distribution of NO_2 internal energy, the internal energy is, on average, to be $\sim 27\,100\ cm^{-1}$, and the average available energy $E_{avail} \sim 3700\ cm^{-1}$.

$$E_{avail} = \left[\sum_{E_{int} > 25\,130\ cm^{-1}} (P_{NO_2}(E_{int}) \times (E_{int} - 25\,130\ cm^{-1}) \right] \div \left(\sum_{E_{int} > 25\,130\ cm^{-1}} [P_{NO_2}(E_{int})] \right). \quad (1)$$

TABLE I. Comparison of vibrational populations of NO $X\ ^2\Pi$ from experimental data and results calculated with prior and SSE models.

Vibrational level NO $X\ ^2\Pi$	Experimental	Prior[a] (1)	Prior[a] (2)	SSE[a] (1)	SSE[a] (2)
0	0.75	0.71	0.77	0.56	0.61
1	0.19	0.21	0.19	0.26	0.28
2	0.07	0.07	0.04	0.12	0.10
3	≈0	0.02	0.01	0.05	0.02

[a](1) and (2) using the internal state distribution of NO_2 from curve (—) and (∘∘∘∘) in Fig. 6, respectively.

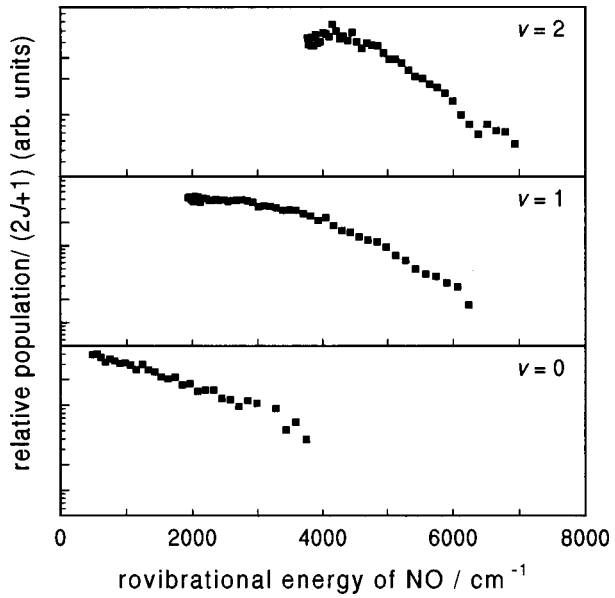

FIG. 5. Boltzmann plots of NO $X\ ^2\Pi$ $v = 0$, 1, and 2 states rovibrational energy of NO.

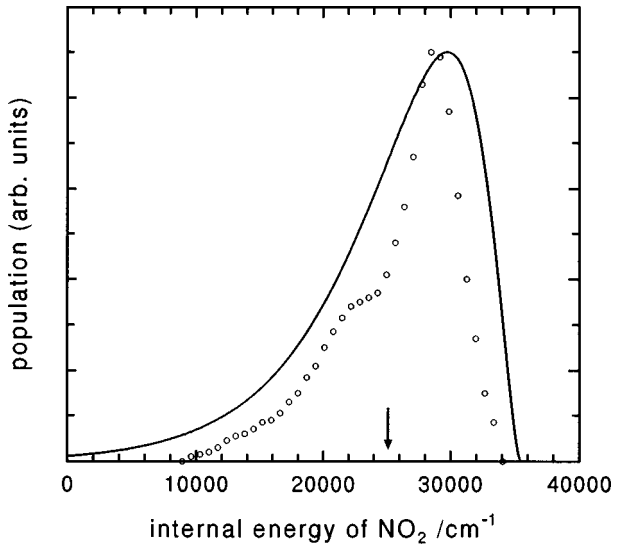

FIG. 6. Distributions of internal energy of fragment NO_2 from nitric acid photolyzed at 193 nm, obtained from subtracting the internal and translational energies of the fragment OH obtained from LIF spectrum of OH[7] (—) and translational energy of products from molecular beam experiment (Ref. 4) (∘∘∘∘), respectively; see text. The position of the arrow shows the dissociation threshold for formation of NO+O.

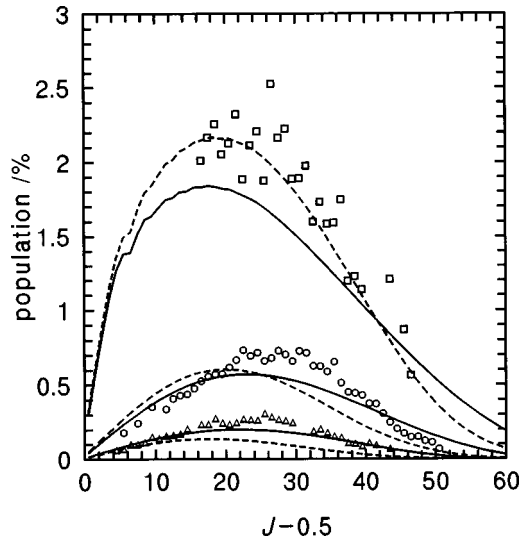

FIG. 7. Plot of experimental distribution of nascent NO $X\ ^2\Pi_{1/2}$ $v=0$, 1, and 2 from photolysis of nitric acid at 193 nm and calculated curves displayed in solid and dashed lines with the prior model using the distributions of internal energy of NO_2 shown in Fig. 6 as (—) and (∘∘∘∘), respectively.

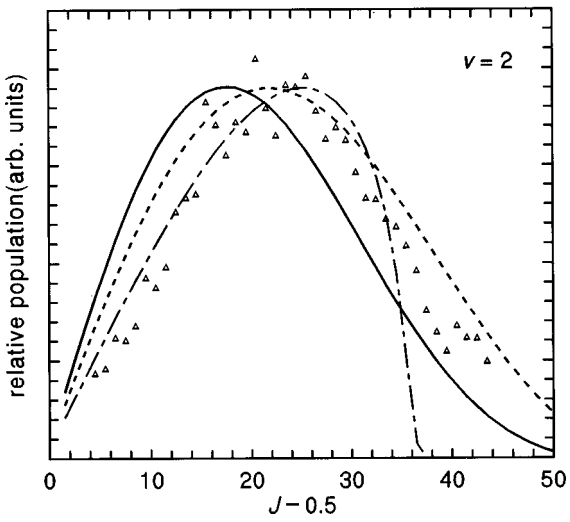

FIG. 8. Plot of rotational distribution of secondary product NO $X\ ^2\Pi_{1/2}$ $v=2$ from experimental data and according to the prior model with internal energy of NO_2 given below: Solid line—distribution obtained from translational energy spectroscopy [shown in Fig. 6 as (∘∘∘∘)], dashed line—distribution obtained from LIF spectrum of OH [shown in Fig. 6 as (—)], and dotted–dashed line—fixed available energy $E_{\text{avail}}=6000\ \text{m}^{-1}$. The calculated curves were scaled on the ordinate axis to obtain a best fit to the experimental distribution.

An oscillatory behavior was observed in the distribution of rotational states of NO dissociated from jet-cooled NO_2 photolyzed with monochromatic light.[16–21,27,28,30–33] Reisler *et al.*[16,17] showed that, on average, these distributions of NO rotational states agree with the calculated results using a statistical model, phase-space theory (PST); this theory is described elsewhere.[17] According to this model both total energy and angular momentum are conserved during dissociation. In our experimental conditions, thermalized nitric acid has a large average rotational angular momentum. Although OH was not produced in highly rotationally excited states, the average rotational angular momentum of NO_2 is expected to be large. In addition, given the broad distribution of internal states of NO_2, the prior model is expected to give results similar to those of the PST. Hence, we used the prior theory that includes no constraint on angular momentum. In Fig. 7 we display a comparison of experimental and calculated prior distributions for three vibrational states given internal energy distributions of NO_2 shown in Fig. 6. For the $v=0$ level, the prior distribution using the internal energy of NO_2 calculated from the translational spectroscopy agrees with the experimental data but not for the other vibrational states. Energetically, the $v=2$ state is dissociated from NO_2 with high internal energy. Hence, we compare the $v=2$ distribution with the calculated distribution shown in Fig. 8 in which the calculated distribution was scaled on the ordinate axis to obtain a best fit to the experimental distribution. As in the case of singlet ketene dissociation,[37] at high available energy the prior model overestimates the NO population for the states of low J and underestimates the population for states with high J. Similar phenomenon is observed for the $v=1$ distribution when compared with the prior distribution. The prior distributions predict the shape of distributions of rotational states of NO incorrectly.

Another statistical model, separated statistical ensemble theory (SSE), was used to calculate the vibrational populations because from the results of Reisler *et al.*[17] the SSE model agrees with experimental data better than the PST. The SSE model assumes the vibrational adiabaticity during the process of dissociation. We used a loose, bending frequency, 100 cm^{-1} suggested by Ionov *et al.*[22] for the transition state of the dissociation channel to form NO+O and the frequency for stretching mode is similar to that of the NO fragment. Both calculated values and experimental data are listed in Table I. The bending mode cannot be treated as an internal rotor in which the SSE model will predict equal population for the vibrational level given a fixed photolysis energy. This will overestimate the vibrational excitation different from the experimental observation.

IV. DISCUSSION

Yeh *et al.*[7] discussed the production mechanism of NO in the ground electronic state from nitric acid photolyzed at 193 nm and concluded that the main mechanism is from NO_2 undergoing secondary dissociation. They reported that the NO was produced within the pulse duration of the excimer laser ≈ 20 ns. Ionov *et al.*[22] And Miyawaki *et al.*[25] have measured directly the apparance of NO at the dissociation threshold of NO_2 to be in the picosecond range. Combining all the results, the secondary dissociation rate of nitric acid is expected to be fast. From the recent results of the transla-

TABLE II. Summary of photodissociation work on NO_2.

E_{avail} (cm^{-1})	v	J	Ω ($^2\Pi_{1/2}/^2\Pi_{3/2}$)	Λ (A'/A'')	Preparation conditions	Reference
1949	72.9% $v=0$, 27.1% $v=1$	Oscillatory	3.4	≈ 1	Jet-cooled	17
1998–2061	79.5% $v=0$, 20.5% $v=1$	Oscillatory	3.4–3	≈ 1	Jet-cooled	17
2200–3038	56%–58% $v=0$, 44%–42% $v=1$	Oscillatory	2.7–2.4	≈ 1	Jet-cooled	17
3360	57% $v=0$, 44% $v=1$	Oscillatory			Jet-cooled	31
7222	44% $v=0$, 28% $v=1$ 16% $v=2$, 12% $v=3$	Oscillatory	1.9	≈ 1	Jet-cooled	32
7336	29% $v=0$, 28% $v=1$, 18% $v=2$, 23% $v=3$, 2.5% $v=4$	Single peaked	1.3–1.9	≈ 1	298 K	11
15 530	Inverted, peaked at $v=5$	$v=0-1$, 3–8 single peaked, $v=2$ double peaked	≈ 1	1.6	Effusive jet	14
This work (0–10 000)	75% $v=0$, 19% $v=1$ 7% $v=2$	$v=0$, 1, 2 Gaussian shaped	1.9	≈ 1	HNO_3	

tional spectroscopy[4] a minor channel of HONO ($\tilde{a}\,^3A''$) production was observed. Larrieu *et al.*[38] performed the quantum chemical calculations and suggested that this excited state correlates to fragment OH+NO without an energy barrier. Hence, HONO ($\tilde{a}\,^3A''$) is expected to be unstable. Kenner *et al.*[39] observed a long-lived intermediate with a lifetime greater than 20 μs from nitric acid after photolysis at 193 nm and assigned this intermediate to be HONO ($\tilde{a}\,^3A''$). Hence, in the time scale of detection used in this work the amount of HONO ($\tilde{a}\,^3A''$) dissociation is expected to be small. Two photon processes like HONO absorbing another 193 nm photon will produce NO. In this work we kept the power of photolysis laser low to be in the linear region to minimize the NO production from these multiphoton processes. Very small amount of NO may be produced via two photon processes, but the major mechanism of NO production is from the unstable NO_2.

Comparison of this work with results obtained on NO_2 dissociation under thermalized and jet-cooled conditions is listed in Table II. Comparing the population ratios of $^2\Pi_{1/2}/^2\Pi_{3/2}$ obtained at various photolytic energies, as the available energy increases this ratio decreases and reaches two. At $E_{avail}=15\,530\ m^{-1}$ the $^2\Pi_{1/2}/^2\Pi_{3/2}$ ratio reaches unity.[14] The production of spin–orbit states in our work was unequal. This experimental ratio $^2\Pi_{1/2}/^2\Pi_{3/2}$, ~ 1.9, agrees with the results of NO from photolysis of NO_2 at low available energy and of theoretical prediction[40] but shows no dependence on the rotational quantum number. According to our work, the two lambda doublet states have about equal population similarly to other results except that at $E_{avail}=15\,530\ m^{-1}$ the population ratio A'/A'' is 1.6.[14]

Under the cold jet conditions of NO_2 the populations of product NO in the ground vibrational level lie between 80%–56% at $E_{avail}=1949-3360\ cm^{-1}$.[17] Our experimental value falls within this range and agrees with those results that the energy distribution in vibrational degrees of freedom behaves statistically. However, our value agrees slightly better with the prior prediction than that of the SSE but the prior model incorrectly predicts the shape of the rotational distributions. The rotational distributions of NO from thermalized NO_2 photolyzed at various wavelengths display singly maxima.[10,11,13] The oscillatory phenomena in the rotational distributions were averaged from contribution of various dissociating NO_2 states. According to the same explanation the oscillatory behavior is expected to be smoothed for NO from nitric acid. At a low available energy, PST was found to predict the averaged rotational distribution correctly, whereas not for large excess energy.[32] Given the shape of the experimental rotational distributions it leads the assumption that at energy greater than the dissociation threshold the distribution of rotational states of NO is resulted from Franck–

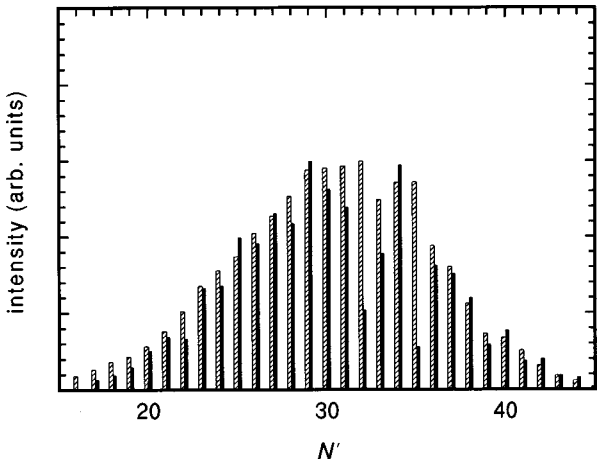

FIG. 9. Stick spectra of emission of the P branch of NO $D\ ^2\Sigma^+ - A\ ^2\Sigma^+$ obtained previously (Ref. 6) (solid stick) and simulated data using experimental population of rotational states of NO $v=1$ obtained in this work (shaded stick). The simulation was done as described previously. (Ref. 7).

Condon overlap of wave functions of the transition state of NO_2 and the rotational state of NO. After summing over all internal states of NO_2, the rotational distributions can be Gaussian-like.[41] This condition explains our observations that the rotational distributions of NO can be fitted with Gaussian functions. At an available energy much in excess of the threshold of dissociation, the position of the transition state can move toward that of the parent molecule and dynamics in the exit channel may determine the product distributions. Similar results were obtained by Knepp *et al.*[32] on photolysis of NO_2 at 309 nm. The SSE calculated with both internal energy distribution of NO_2 seems to slightly overestimate the vibrational excitation. These results imply that the prior model without considering the adiabaticity of vibrational energy of NO works properly in this case.

Myers *et al.*[4] reported that unstable NO_2 which dissociates to NO+O is in none of the lowest four electronic states nor in a quartet state. When NO_2 is excited with a photon in the range 350–400 nm, the dissociating states are considered to have characters of mixed $^2B_2$ and $^2A_1$ states, because of strong vibronic coupling between these two lowest electronic states. From agreement between distributions of internal states of NO from nitric acid with NO_2 after photolysis, our data imply that the dissociating channel underwent fragmentation via the ground electronic surface. The unstable NO_2 is expected to be in an electronic state that couples strongly to the ground electronic surface. Hence, in the case of dissociation of nitric acid, even NO is a secondary product; the distributions of internal states can be understood from dynamics obtained from the experiments using cold molecular jets.

We used the population obtained in this work to simulate the emission spectrum of NO $D\ ^2\Sigma^+ - A\ ^2\Sigma^+$ obtained in this group previously[7] via time-resolved Fourier-transform spectroscopy. The method of simulation was described previously.[7] Both spectra agree well (Fig. 9) and confirm the results observed previously that the NO emission is the state $X\ ^2\Pi\ v=1$ state absorbing a 193 nm photon. In the experimental spectrum, the low spectral intensities for $N'=32$ and 35 occur because these $D\ ^2\Sigma^+$ states are perturbed.[42] The small oscillatory phenomenon observed previously in the relative spectral intensities of even and odd parity states of NO, are not confirmed in the present work. With LIF the uncertainty is greater than that obtained using a time-resolved Fourier-transform spectrometer in determining the relative spectral intensity of rotational states. However, other factors excluded from the simulation may contribute intensity variation in even–odd parity states.[7]

ACKNOWLEDGMENTS

The authors thank L. J. Butler for providing a preprint, and National Science Council of the Republic of China (Contract No. NSC 86-2113-M-007-38) for support.

[1] A. A. Turnipseed, G. L. Vaghijani, J. E. Thompson, and A. R. Ravishankara, J. Chem. Phys. **96**, 5887 (1992).
[2] A. Schiffman, D. D. Nelson, Jr., and D. J. Nesbitt, J. Chem. Phys. **198**, 6935 (1993).
[3] P. Felder, X. Yang, and J. R. Huber, Chem. Phys. Lett. **215**, 221 (1993).
[4] T. L. Myers, N. Forde, D. C. Kitchen, B. Hu, and L. J. Butler, J. Chem. Phys. **107**, 5361 (1997).
[5] JANAF Thermochemical Tables, J. Phys. Chem. Ref. Data, Suppl. **14**, (1985).
[6] U. Robra, H. Zacharias, and K. H. Welge, Z. Phys. D **16**, 175 (1990).
[7] P.-S. Yeh, G.-H. Leu, Y.-P. Lee, and I-C. Chen, J. Chem. Phys. **103**, 4879 (1995).
[8] G.-H. Leu, C.-W. Hwang, and I-C. Chen, Chem. Phys. Lett. **257**, 481 (1996).
[9] Y. Y. Bai and G. A. Segal, J. Chem. Phys. **92**, 7479 (1990).
[10] H. Zacharias, M. Geilhaupt. K. Meier, and K. H. Welge, J. Chem. Phys. **74**, 218 (1981).
[11] H. Zacharias, K. Meier, and K. H. Welge, *Energy Storage and Redistribution in Molecules*, edited by J. Hinze (Plenum, New York, 1983), p. 107.
[12] M. Mons and I. Dimicoli, Chem. Phys. Lett. **131**, 298 (1986).
[13] M. Mons and I. Dimicoli, Chem. Phys. **130**, 307 (1989).
[14] J. McFarlane, J. C. Polanyi, and J. G. Shapter, J. Photochem. Photobiol. A: Chem. **58**, 139 (1991).
[15] J. Miyawaki, K. Yamanouchi, and S. Tsuchiya, Chem. Phys. Lett. **180**, 287 (1991).
[16] D. C. Robie, M. Hunter, J. L. Bates, and H. Reisler, Chem. Phys. Lett. **193**, 413 (1992).
[17] M. Hunter, S. A. Reid, D. C. Robie, and H. Reisler, J. Chem. Phys. **99**, 1093 (1993).
[18] S. A. Reid, J. T. Brandon, M. Hunter, and H. Reisler, J. Chem. Phys. **99**, 4860 (1993).
[19] N. Changlong, L. Hua, and J. Pfab, J. Chem. Phys. **97**, 7458 (1993).
[20] J. Miyawaki, K. Yamanouchi, and S. Tsuchiya, J. Chem. Phys. **99**, 254 (1993).
[21] V. P. Hradil, T. Suzuki, S. A. Hewitt, P. L. Houston, and B. J. Whitaker, J. Chem. Phys. **99**, 4455 (1993).
[22] S. I. Ionov, G. A. Brucker, C. Jaques, Y. Chen, and C. Wittig, J. Chem. Phys. **99**, 3420 (1993).
[23] S. J. Klippenstein and T. Radivoyevitch, J. Chem. Phys. **99**, 3644 (1993).
[24] C. Wittig and S. I. Ionov, J. Chem. Phys. **100**, 4714 (1994).
[25] J. Miyawaki, K. Yamanouchi, and S. Tsuchiya, J. Chem. Phys. **100**, 4716 (1994).
[26] S. I. Ionov, H. F. Davis, K. Mikhaylichenko, L. Valachovic, R. A. Beaudet, and C. Wittig, J. Chem. Phys. **101**, 4809 (1994).
[27] S. A. Reid and H. Reisler, J. Chem. Phys. **101**, 5683 (1994).
[28] S. A. Reid, D. C. Robie, and H. Reisler, J. Chem. Phys. **100**, 4256 (1994).
[29] S. A. Reid and H. Reisler, J. Chem. Phys. **101**, 5683 (1994).
[30] J. Miyawaki, K. Yamanouchi, and S. Tsuchiya, J. Chem. Phys. **101**, 4505 (1994).
[31] J. A. Harrison, X. Yang, M. Rösslein, P. Felder, and J. R. Huber, J. Phys. Chem. **98**, 12260 (1994).
[32] P. T. Knepp, A. C. Terentis, and S. H. Kable, J. Chem. Phys. **103**, 194 (1995).
[33] S. A. Reid, D. C. Robie, and H. Reisler, J. Phys. Chem. **100**, 474 (1996).
[34] C. Wittig, I. Nadler, H. Reisler, M. Noble, J. Catanzarite, and G. Radhakrishnan, J. Chem. Phys. **83**, 5581 (1985).
[35] L. T. Earls, Phys. Rev. **48**, 423 (1935).
[36] H. Scheingraber and C. R. Vidal, J. Opt. Soc. B **2**, 343 (1985).
[37] E. A. Wade, H. Clauberg, S. K. Kim, A. Mellinger, and C. B. Moore, J. Chem. Phys. A **101**, 732 (1997).
[38] C. Larrieu, A. DarGelos, and M. Chaillet, Chem. Phys. Lett. **91**, 465 (1982).
[39] R. D. Kenner, F. Rohrer, Th. Papenbrock, and F. Stuhl, J. Phys. Chem. **90**, 1294 (1986).
[40] H. Katagiri and S. Kato, J. Chem. Phys. **99**, 8805 (1993).
[41] R. Schinke, *Photodissociation Dynamics* (Cambridge University Press, Cambridge, 1993).
[42] E. Miescher, J. Chem. Phys. **73**, 3088 (1980).